Appl Biochem Biotechnol (2010) 160:561–573
DOI 10.1007/s12010-008-8430-x

Study of Phase Transformation of Guanosine 5′-Monophosphate in Drowning-Out Crystallization

Jeongki Kang · Nguyen Anh Tuan · Jong-Min Kim · Sang-Mok Chang · Woo-Sik Kim

Received: 16 March 2008 / Accepted: 3 November 2008 /
Published online: 25 November 2008

Abstract The present study used a mechanistic approach to control the phase transformation of guanosine 5′-monophosphate (GMP) via the operating conditions of agitation and feed concentration during drowning-out crystallization. First, Fourier transform infrared and UV/vis spectrophotometry were successfully applied to monitor the mass fraction of GMP polymorphs (amorphous and hydrate crystalline GMPs) and GMP supersaturation, respectively, during the crystallization. The phase transformation of amorphous GMP into hydrate crystals was significantly influenced by the agitation, which promoted the mass transfer of GMP dissolution and growth. Therefore, the phase transformation was quickly finished when increasing the agitation speed. However, a high agitation caused breakage of the hydrate crystals, resulting in a reduced crystal size with a bimodal distribution. The phase transformation was also influenced by the GMP feed concentration, as the crystal growth was promoted and the crystal size increased when increasing the feed concentration up to 61 g/l. However, a further increase in the feed concentration caused secondary nucleation due to the induction of a high supersaturation level during the phase transformation, leading to a small crystal size with a bimodal distribution. In addition, the rectangular-shaped hydrate GMP crystals exhibited a higher growth rate in the b direction rather than the a direction. Therefore, the crystal morphology shifted from a long rectangle to a square when increasing the feed concentration.

Keywords Guanosine 5′-monophosphate · Phase transformation · Drowning-out crystallization · Polymorphs

J. Kang · N. A. Tuan · W.-S. Kim (✉)
Department of Chemical Engineering, Kyunghee University, Kyungki-do 449-701, Korea
e-mail: wskim@khu.ac.kr

J.-M. Kim · S.-M. Chang
Department of Chemical Engineering, Dong-A University, Busan 314-701, Korea

Introduction

The polymorphism of organic compounds is of great interest to industrial crystallization, especially in the areas of food, pharmaceuticals, and fine chemicals, as the physicochemical properties of solubility, density, stability, and bioavailability depend directly on the polymorphs [1–4]. Thus, many studies have focused on polymorphism and phase transformation in order to obtain the required crystal phase during crystallization.

A good example is taltirelin, which can only be used as a pharmaceutical drug in an α-form crystal due to its bioavailability. Therefore, the polymorphic control and phase transformation of taltirelin have been intensively studied by Maruyama and Ooshima [5–7] who identified the operating conditions of the additive, temperature, seeding, and agitation speed in the cooling crystallization as critical factors to control the polymorph. They also found that the dissolution of the metastable form (α-form) was a rate-determining step in the phase transformation when they measured the dissolution rate of the α-form crystal along with the methanol additive. Similarly, in the crystallization of mefenamic acid, the humidity and seed have been identified as the determining factors for the polymorphism [8]. Meanwhile, many other conditions, including the pH, solvent species and composition, solvent evaporation rate, solute concentration, and impurities have also been investigated to determine the polymorphs, crystal shape, crystal size, and crystal purity during crystallization [9–12].

In the crystallization of inorganic substances, calcium carbonate has been the frequent focus for polymorphic studies, as it has three kinds of crystalline polymorph: calcite, aragonite, and vaterite, plus one amorphous phase. According to Kim et al. [13], in the crystallization reaction, amorphous calcium carbonate is initially precipitated and transformed into vaterite, then finally changed into stable calcite. Their study also showed that the phase transformation was significantly controlled by the pH and initial supersaturation. Meanwhile, in the case of calcium carbonate crystallization in a reverse micelle, the anionic surfactants of sodium dodecyl sulfate and sodium bis(2-ethylhexyl) sulfosuccinate have been found to be highly effective in preventing the phase transformation of vaterite into calcite [14]. In addition, bio-proteins have been used to control the polymorphs of calcium oxalate crystals [15].

However, in contrast to such previous studies, the present study applied a mechanistic approach to control the phase transformation during the drowning-out crystallization of guanosine 5′-monophosphate (GMP). Thus, since the phase transformation in a solution is known to be performed via dissolution and growth, the agitation and feed concentration were considered as the key operation conditions to investigate the phase transformation of GMP.

Experiments

GMP hydrate crystals supplied from Cheil Jedang Co. (99% purity) were used for the drowning-out crystallization without further purification. The GMP feed solution was prepared by dissolving the GMP hydrate crystals into distilled water. In a standard mixing crystallizer with a 0.5-l working volume, 250 ml of the GMP feed solution was initially loaded, then the same volume (250 ml) of an anti-solvent (methanol, ACS grade) was instantaneously injected into the crystallizer to induce crystallization. The crystallizer was made of Pyrex glass equipped with a propeller-type agitator. The crystallization conditions of the agitation speed and initial GMP concentration were varied from 200 to 1,000 rpm and from 30.5 to 122 g/l, respectively. The temperature of the crystallization was always fixed at 25 °C.

To monitor the crystallization, the suspension was intermittently sampled to analyze the structure of the GMP products and GMP concentration using an X-ray diffraction (XRD; Mac Science, M18XHF-SRA, Japan) and UV/vis spectrophotometer (JASCO, V-570, Japan). About 10-ml samples were taken and quickly filtered using a vacuum, then the solid product was dried in an oven for analysis. Plus, Fourier transform infrared (FT-IR; PERKIN ELMER, SYSTEM 2000 FT-IR, USA) was used to measure the polymorphic fraction of the GMP products and an optical video-microscope (Sometech Co., STVMS 305R, Korea) used to determine the crystal size and shape.

Results and Discussion

When conducting the drowning-out crystallization of GMP at room temperature, two polymorphs of GMP, an amorphous solid and crystalline hydrate, were generally encountered, as shown in Fig. 1. Using TGA, the resulting crystalline GMP was confirmed as a 7-hydrate. First, a standard calibration curve of the polymorphic fraction was prepared using reference solids of amorphous GMP and 7-hydrate GMP crystals, as shown in Fig. 2. According to the FT-IR, the characteristic peaks of the GMP were found at 1,540 and 1,690 cm^{-1}, which originated from C=C and C=O stretchings of the GMP molecule, respectively. Furthermore, since the intensities were directly dependent on the molecular arrangement in the solid state, this allowed the mass fraction of the GMP polymorphs to be calibrated in terms of the characteristic peak intensities (Fig. 2b). This standard curve was then used to estimate the polymorphs in the solid crystallization products. Similarly, to monitor the GMP concentration in the solution, a standard calibration was prepared using a UV/vis spectrophotometer (not shown in the manuscript).

The dynamic behavior of the GMP drowning-out crystallization, including the supersaturation of the solution, crystallinity of the solid product, and mean crystal size of the suspension were all monitored in the batch crystallizer, as shown in Fig. 3. The spontaneous crystallization of GMP was induced by the injection of an anti-solvent into the GMP solution. Initially, metastable solids (amorphous GMP) was formed due to the high supersaturation. The supersaturation level was then quickly reduced to the solubility of the amorphous GMP (called the metastable solubility; 13.1 g/l) and continued to decrease gradually to the solubility of the GMP hydrate crystals (called the stable solubility; 9.5 g/l;

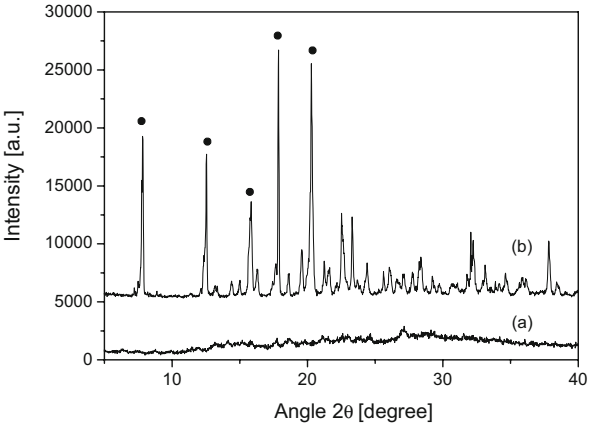

Fig. 1 Typical powder pattern XRD peaks of amorphous and crystalline GMP solids. **a** Amorphous GMP, **b** hydrate GMP crystals

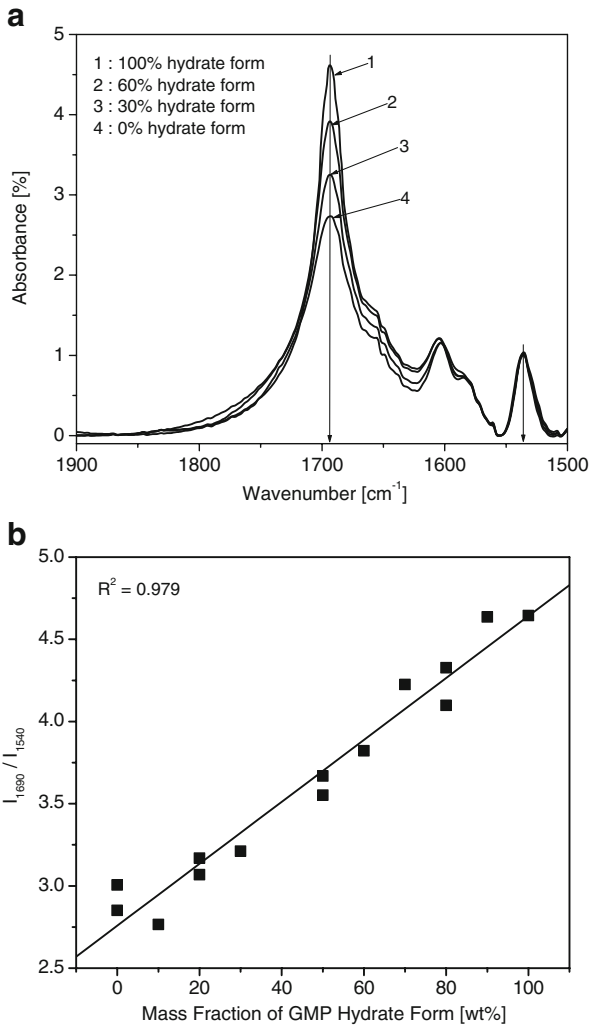

Fig. 2 FT-IR analysis of polymorphic mixture: **a** Characteristic peaks of mixture of amorphous GMP and hydrate GMP crystal and **b** calibration of mass fraction of polymorphs using characteristic peak intensities

Fig. 3a). In the metastable supersaturation between the metastable and stable solubilities, the amorphous GMP were dissolved and recrystallized into stable ones (7-hydrate GMP crystals), referred to as the phase transformation. In the present crystallization study, the dynamic profile of the supersaturation was found to depend significantly on the agitation speed. As such, at an agitation speed of 200 rpm, it took about 250 min for the supersaturation level to reach the stable solubility, where this time period was counted as phase transformation time. However, this phase transformation time was dramatically reduced to about 120 min with a high agitation speed of 600 rpm, meaning that the phase transformation became faster when increasing the agitation speed. Meanwhile, the feed concentration of GMP exhibited no apparent influence on the phase transformation time.

The dependency of the GMP solid product on the agitation and feed concentration appeared to be similar to that of the supersaturation (Fig. 3b). As such, the dynamic profile of the GMP solid product indicated that the initial GMP precipitate was mostly composed of amorphous solid and was transformed into the crystalline hydrate during the

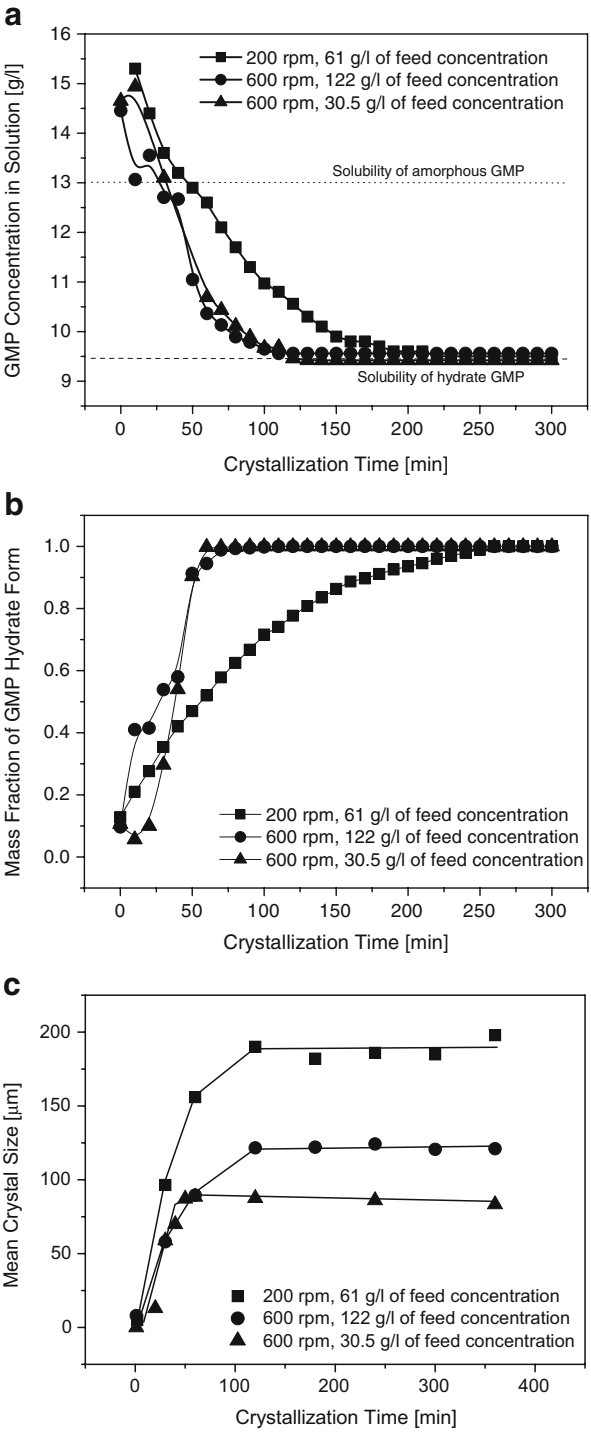

Fig. 3 Dynamic behavior of GMP crystallization: Dynamic profile of GMP concentration during crystallization (**a**), dynamic profile of mass fraction of hydrate GMP crystal in product solid during crystallization, and **c** dynamic profile of mean crystal size during crystallization (**b**)

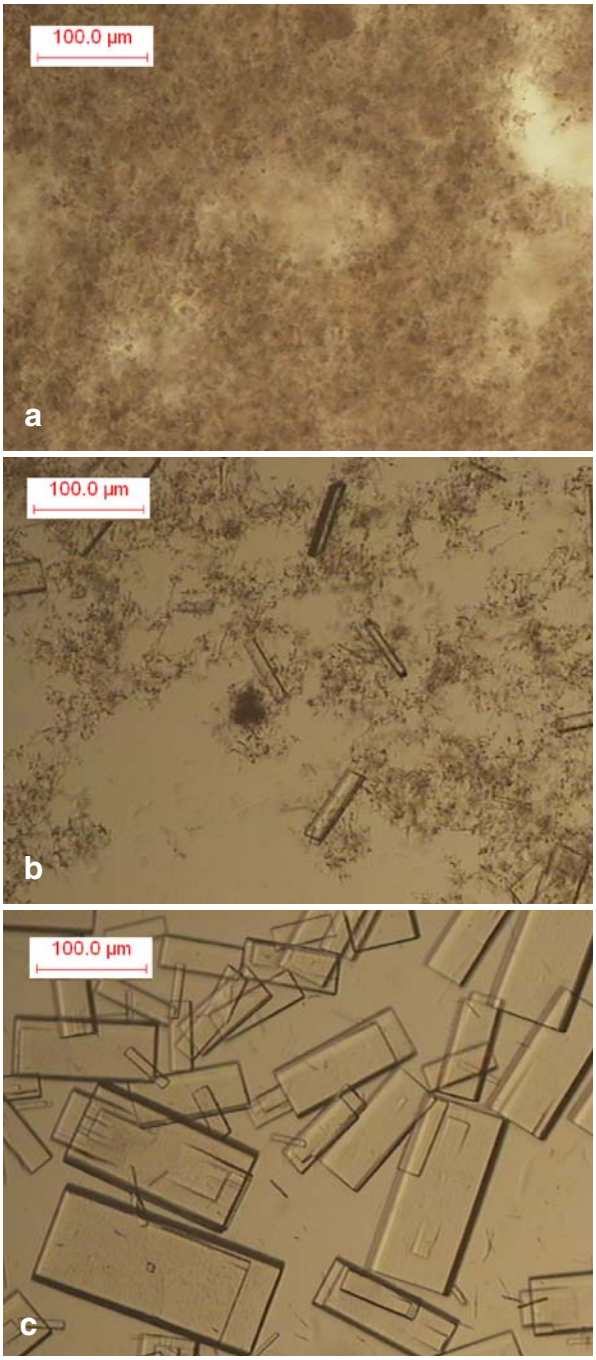

Fig. 4 Typical morphological change of GMP solids during crystallization with 122 g/l feed concentration and 600 rpm agitation speed: Crystallization time= 0 min (**a**), crystallization time= 10 min (**b**), and crystallization time=120 min (**c**)

crystallization. Then, the mass fraction of GMP hydrate crystals in the solid product approached 100% as the superaturation reached at the stable solubility. When compared with the above dynamic profile of the supersaturation, it can be inferred that GMP hydrate crystals were already nucleated at a supersaturation above the metastable solubility and grew via the transformation of

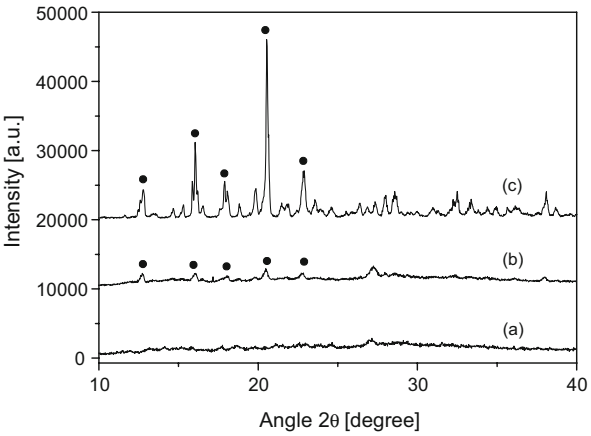

Fig. 5 Typical structural shift of GMP solids during crystallization with 122 g/l feed concentration and 600 rpm agitation speed: crystallization time=0 min (**a**), crystallization time=10 min (**b**), and crystallization time=120 min (**c**)

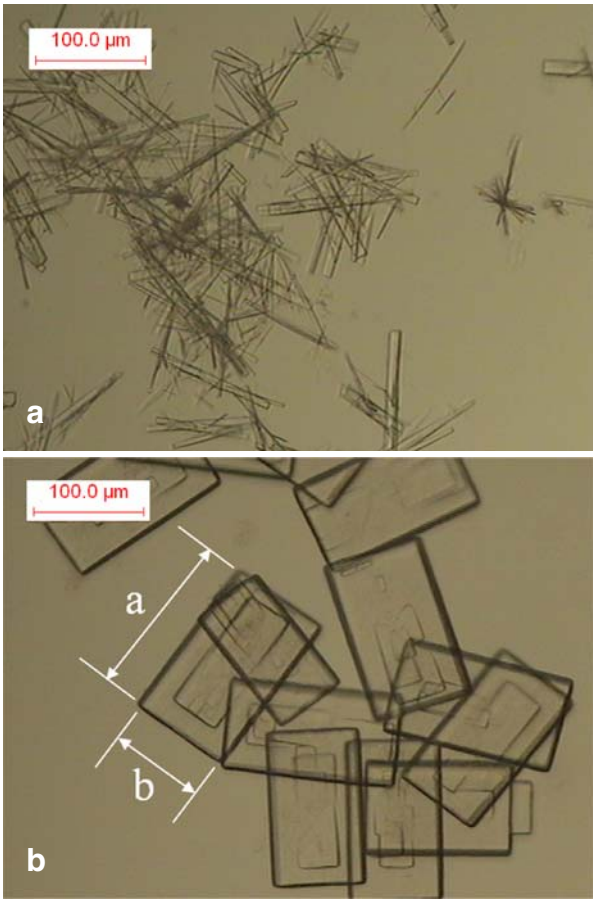

Fig. 6 Typical morphology of hydrate GMP crystals at end of crystallization: GMP crystals with 30.5 g/l feed concentration and 600 rpm agitation speed (**a**), GMP crystals with 61 g/l feed concentration and 600 rpm agitation speed (**b**), GMP crystals with 122 g/l feed concentration and 600 rpm agitation speed (**c**), and GMP crystals with 61 g/l feed concentration and 1000 rpm agitation speed (**d**)

Fig. 6 (continued)

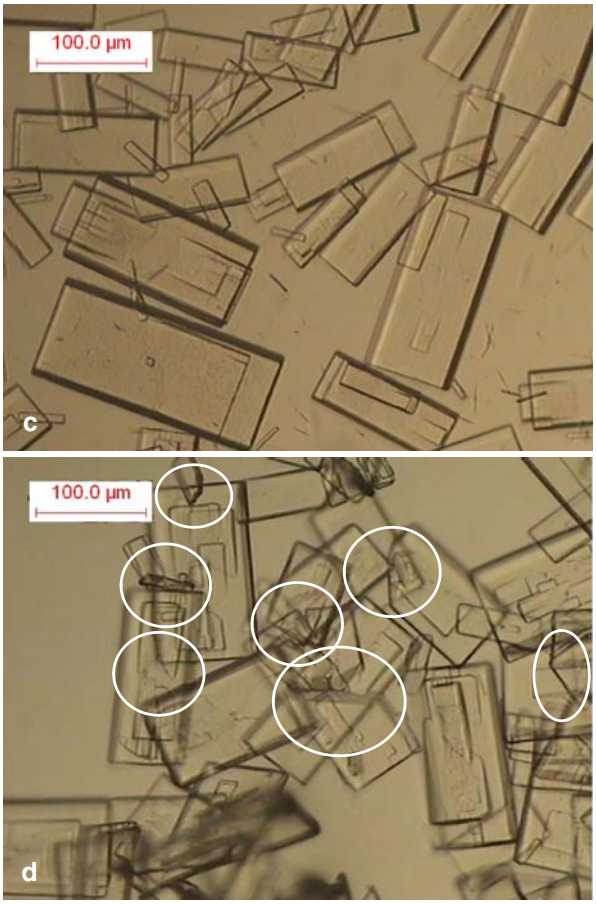

the amorphous GMP. In addition, the phase transformation of amorphous GMP to hydrate crystals was facilitated with a higher agitation speed due to promotion of the dissolution of the amorphous GMP and growth of the hydrate crystals. Furthermore, the dynamic profiles of the mean size of the GMP hydrate crystals also revealed that the crystal nucleation and growth were strongly influenced by the agitation speed and feed concentration (Fig. 3c).

The microscopic observation of the GMP solids during the crystallization was well matched with the above dynamic behavior of the GMP crystallization, as shown in Fig. 4. During the initial stage of the crystallization, the precipitate of the GMP solid was clearly seen to be amorphous, which was also confirmed by powder XRD (Fig. 4a). However, after 10 min, the formation of GMP hydrate crystals was observed (Fig. 4b). Via the phase transformation, the amorphous GMP was dissolved and recrystallized as hydrate crystals, resulting in a complete disappearance of amorphous GMP after 120 min of crystallization time (Fig. 4c). Also, the structural shift of the GMP solids during the phase transformation were confirmed by XRD, as displayed in Fig. 5.

As a result of the crystallization, the final solid product of GMP hydrate crystals was generally rectangular in shape, as shown in Fig. 6. However, the shapes and sizes varied according to the agitation speed and feed concentration. At a low feed concentration (30.5 g/l), the GMP crystals were small and shaped like a needle (Fig. 6a), while increasing

the feed concentration produced rectangular crystals with a uniform size (Fig. 6b), and a further increase in the feed concentration resulted in a wide crystal size distribution (Fig. 6c). In the case of a high agitation speed of 1,000 rpm, crystal fractures were also observed (circled in Fig. 6d).

For a quantitative description of the GMP crystal morphology, the crystal size was counted as the length of the rectangles ("a" in Fig. 6b), while the crystal shape factor was defined as the ratio of the length (a) to the width (b) of the rectangles. As shown in Fig. 7, the crystal size was reduced from 200 to 120 μm when increasing the agitation speed, which may have been due to crystal breakage by collisions, thereby increasing the crystal population and reducing the mean crystal size when increasing the agitation speed. Crystal breakage was evident from crystal fractures (Fig. 7d) and the bimodal crystal size distribution (Fig. 7b). However, the shape factor of the crystals was almost independent of the agitation speed.

As mentioned above, since the drowning-out crystallization of GMP solids was quickly induced by injection of anti-solvent, the time period to complete the crystallization (called the completion time) was mostly taken by the phase transformation of the amorphous GMP into hydrate crystals. Thus, the completion time was reduced from 250 to 110 min when increasing the agitation speed from 200 to 1,000 rpm due to the promotion of the dissolution and growth processes in the phase transformation, as shown in Fig. 8.

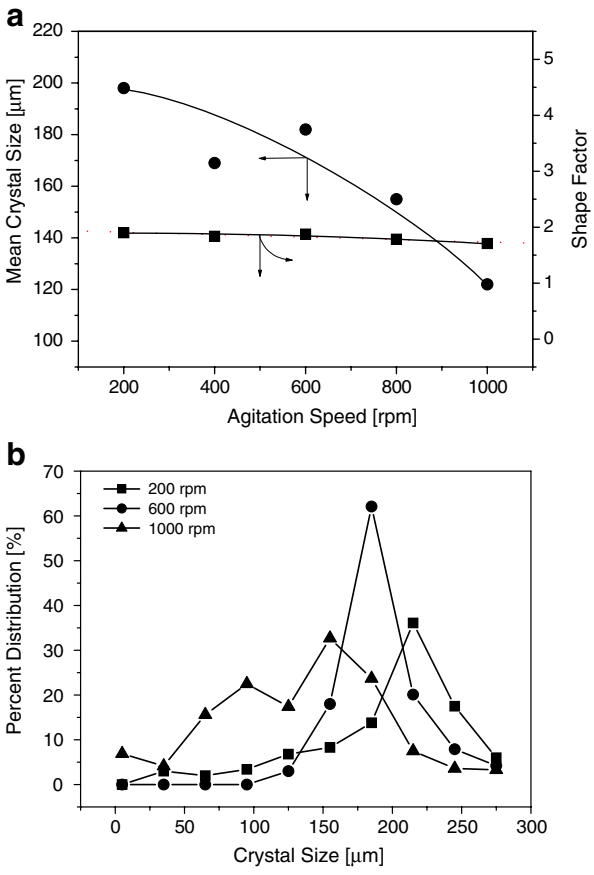

Fig. 7 Influence of agitation speed on GMP crystallization at 61 g/l of feed concentration: mean crystal size and crystal shape factor (**c**) and crystal size distribution (**b**)

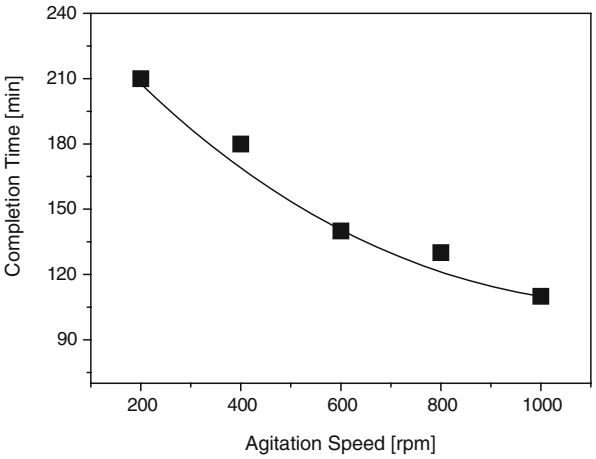

Fig. 8 Influence of agitation speed on completion time of GMP crystallization at 61 g/l of feed concentration

Meanwhile, the GMP feed concentration was found to have a distinct influence on the mean crystal size, crystal shape, and completion time compared to the agitation speed, as shown in Figs. 9 and 10. More amorphous GMP was precipitated when increasing the feed concentration, resulting in a higher supersaturation level in the metastable region due to the enhanced surface area of amorphous GMP for the dissolution process. In other words, the supersaturation level in the metastable region was determined by the balance between the generation of the supersaturation by the amorphous GMP dissolution and the consumption of the supersaturation by the GMP crystal growth, and both generation and consumption rates of the supersaturation depended on the surface areas of amorphous and crystal GMPs. Thus, at a higher feed concentration, a more amorphous GMP initially crystallized supplied a larger surface area for the dissolution. Here, the supersaturation generated by the dissolution would mostly be consumed for the crystal growth without a secondary nucleation if the surface area of GMP crystal were large enough. However, the further increase of the feed concentration would precipitate a more amorphous GMP increasing the generation rate of supersaturation than its consumption rate, inducing the secondary nucleation of GMP crystals for additional consumption of the supersaturation in the metastable region. Thereby, it might be considered that below 61 g/l of the feed concentration, the increase of the feed concentration provided the higher driving force for the growth of the GMP crystals without a serious secondary nucleation, resulting in the larger crystal mean size of up to 190 μm. However, when further increasing the feed concentration above 61 g/l, the generation rate of the supersaturation by dissolution of the amorphous GMP surpassed the consumption rate of the supersaturation by growth of GMP crystals. Thus, the higher supersaturation level was built up in the metastable region, causing the simultaneous promotion of crystal growth and secondary nucleation, thereby reducing the mean crystal size, as shown in Fig. 9a. Such an influence of the feed concentration on the supersaturation level in the metastable region could be hinted from the dynamic profiles of the superstation in Fig 3a. At 122 g/l of the feed concentration, the supersaturation level after the initial rapid drop was maintained near the metastable solubility level for about 30 min (from 10 to 40 min in crystallization time) to nucleate the secondary GMP crystals, whereas it was monotonically reduced at the low feed concentrations of 30.5 and 61 g/l. These assumptions were also confirmed from the crystal size distribution shown in Fig. 9b. As such, with a feed concentration below 61 g/l, the mono-mode crystal size distribution shifted to the right when increasing the feed

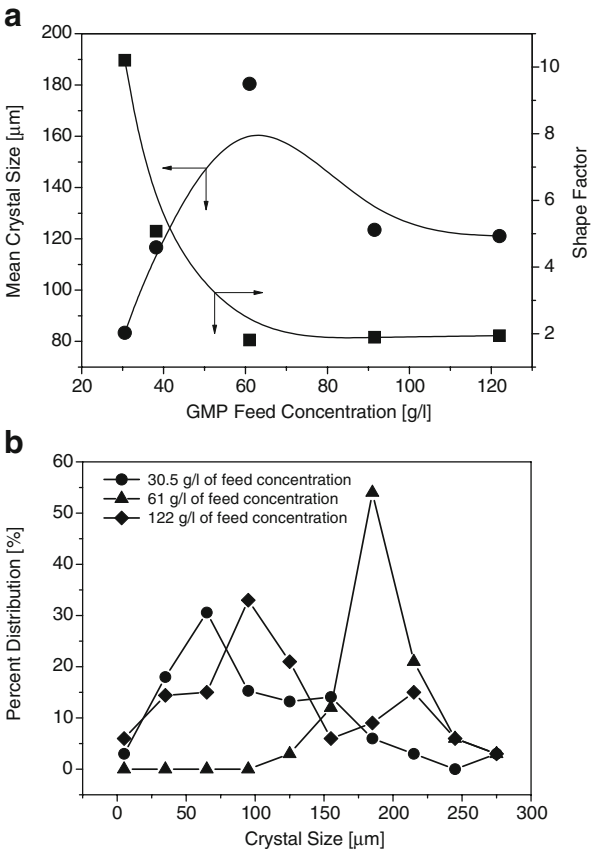

Fig. 9 Influence of feed concentration on GMP crystallization at 600 rpm of agitation speed: mean crystal size and crystal shape factor (**a**) and crystal size distribution (**b**)

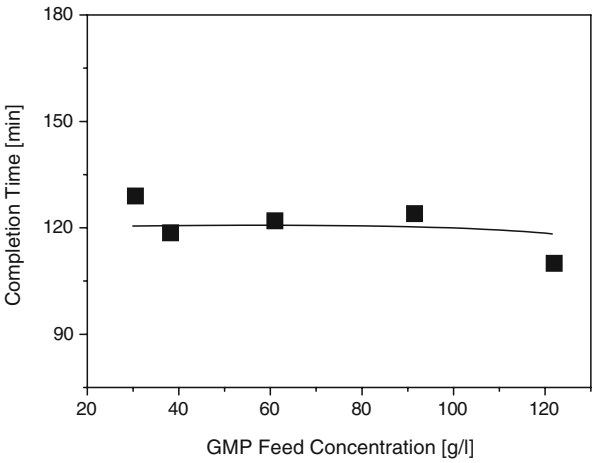

Fig. 10 Influence of feed concentration on completion time of GMP crystallization at 600 rpm of agitation speed

concentration, yet increasing the feed concentration above 60 g/l resulted in a bimodal distribution with a high population of small crystal sizes, presumably formed by the secondary nucleation.

The crystal shape factor was also monotonically reduced when increasing the feed concentration (Fig. 9a), inferring that the crystal growth rate was significantly more promoted in the b direction rather than in the a direction when increasing the supersaturation level using the feed concentration. A different directional growth of the crystal face according to the supersaturation level was also previously observed in paracetamol [16]. Although the amount of precipitated amorphous GMP increased when increasing the feed concentration, it was consistently consumed by the promoted crystal growth and secondary nucleation. Therefore, as shown in Fig. 10, the completion time appeared to be almost independent of the feed concentration, although a slight reduction was noted with a high feed concentration of 122 g/l due to the further acceleration of the phase transformation as a result of the high population of crystals produced via the secondary nucleation.

Conclusion

The present work revealed that the agitation speed and GMP feed concentration both had a significant effect on the drowning-out crystallization of GMP. Since amorphous GMP was spontaneously precipitated by the injection of an anti-solvent into the GMP feed solution, the influence of the agitation speed and feed concentration was mostly related to the phase transformation of the amorphous GMP into hydrate crystals. The amorphous GMP dissolution and hydrate crystal growth were both promoted by the agitation speed, resulting in a reduced completion time, plus the mean crystal size was reduced when increasing the agitation primarily due to breakage of the hydrate crystals.

In contrast, the GMP feed concentration had little influenced on the completion time, as the mass transfer coefficients of dissolution and growth were apparently independent of the feed concentration. However, increasing the feed concentration up to 61 g/l induced a higher supersaturation level, resulting in a larger crystal size with a mono-modal distribution. Yet, the higher supersaturation with a further increase in the feed concentration induced secondary nucleation, resulting in a small crystal size with a bimodal distribution. In addition, due to the different directional growth of the crystal face, the crystal shape factor was reduced when increasing the feed concentration.

In conclusion, the present study showed that the phase transformation of GMP during drowning-out crystallization was predominantly controlled by the crystallization conditions of the agitation speed and feed concentration.

Acknowledgment This study was financially supported by KEMCO (2006-11-0200-3-010).

References

1. Hartel, R. W. (2001). *Crystallization in foods* (1st ed.). Maryland, US: Aspen.
2. Hilfiker, R. (2006). *Polymorphism* (1st ed.). Basel, Switzerland: Wiley-VCH.
3. Mullin, J. W. (2001). *Crystallization* (4th ed.). Woburn, USA: Butterworth-Heinemann.
4. Tavare, N. S. (1995). *Industrial crystallization* (1st ed.). Manchester, UK: Springer.
5. Maruyama, S., Ooshima, H., & Kato, J. (1999). *Chemical Engineering Journal*, *75*, 193–200. doi:10.1016/S1385-8947(99)00115-1.

6. Maruyama, S., & Ooshima, H. (2000). *Journal of Crystal Growth*, *212*, 239–245. doi:10.1016/S0022-0248(99)00903-3.
7. Maruyama, S., & Ooshima, H. (2001). *Chemical Engineering Journal*, *81*, 1–7. doi:10.1016/S1385-8947(00)00193-5.
8. Kato, F., Otsuka, M., & Matsuda, Y. (2006). *International Journal of Pharmaceutics*, *321*, 18–26. doi:10.1016/j.ijpharm.2006.04.020.
9. Sheikhzadeh, M., Murad, S., & Rohani, S. (2007). *Journal of Pharmaceutical and Biochemical Analysis*, *45*, 227–236. doi:10.1016/j.jpba.2007.06.001.
10. Shan, G., Igarashi, K., Noda, H., & Ooshima, H. (2002). *Chemical Engineering Journal*, *85*, 169–176. doi:10.1016/S1385-8947(01)00154-1.
11. Kitamura, M., Hara, T., & Takimoto-Kamimura, M. (2006). *Crystal Growth & Design*, *6*, 1945–1950. doi:10.1021/cg050464e.
12. Lee, M. H., Kim, J. H., Park, Y. C., & Kim, W.-S. (2007). *Industrial & Engineering Chemistry Research*, *46*, 1500–1504. doi:10.1021/ie0608152.
13. Kim, W. S., Hirasawa, I., & Kim, W.-S. (2004). *Industrial & Engineering Chemistry Research*, *43*, 2650–2657. doi:10.1021/ie034161y.
14. Kang, S. H., Choi, C. K., Hirasawa, I., & Kim, W.-S. (2005). *Journal of Colloid and Interface Science*, *288*, 496–502. doi:10.1016/j.jcis.2005.03.015.
15. Jung, T., Choi, C. K., & Kim, W.-S. (2005). *Journal of Crystal Growth*, *279*, 154–162. doi:10.1016/j.jcrysgro.2005.02.010.
16. Davey, R., & Garside, J. (2003). *From molecules to crystallizers: An introduction to crystallization*. Oxford, UK: Oxford Science Publications.